SLAC-PUB-7216
ICHEP-96 PA07-065
ICHEP-96 PA07-066
July/22/96

Tau Lorentz Structure with Polarization at SLD *

The SLD Collaboration**
Stanford Linear Accelerator Center
Stanford University, Stanford, CA 94309

Abstract

We present a measurement of the tau neutrino helicity (h_{ν_τ}) and the Michel parameters (ρ, ξ and δ) by analyzing the τ decays $\tau \rightarrow \pi(\mathrm{K})\nu_\tau$, $\tau \rightarrow \mathrm{e}\bar{\nu}_e\nu_\tau$ and $\tau \rightarrow \mu\bar{\nu}_\mu\nu_\tau$ in $e^+e^- \rightarrow Z^0 \rightarrow \tau^+\tau^-$. The analysis uses the 1993-1995 SLD data sample of 4316 τ-pair events produced with highly polarized electrons. We obtain preliminary results of $\mathrm{h}_{\nu_\tau} = -0.81 \pm 0.18 \pm 0.03$, $\rho = 0.71 \pm 0.09 \pm 0.04$, $\xi = 1.03 \pm 0.36 \pm 0.05$ and $\xi\delta = 0.84 \pm 0.27 \pm 0.05$.

Paper Contributed to the XXVIII International Conference on High Energy Physics, July/96, Warsaw, Poland

*This work was supported by Department of Energy contracts: DE-FG02-91ER40676 (BU), DE-FG03-92ER40701 (CIT), DE-FG03-91ER40618 (UCSB), DE-FG03-92ER40689 (UCSC), DE-FG03-93ER40788 (CSU), DE-FG02-91ER40672 (Colorado), DE-FG02-91ER40677 (Illinois), DE-AC03-76SF00098 (LBL), DE-FG02-92ER40715 (Massachusetts), DE-AC02-76ER03069 (MIT), DE-FG06-85ER40224 (Oregon), DE-AC03-76SF00515 (SLAC), DE-FG05-91ER40627 (Tennessee), DE-FG02-95ER40896 (Wisconsin), DE-FG02-92ER40704 (Yale); National Science Foundation grants: PHY-91-13428 (UCSC), PHY-89-21320 (Columbia), PHY-92-04239 (Cincinnati), PHY-88-17930 (Rutgers), PHY-88-19316 (Vanderbilt), PHY-92-03212 (Washington); the UK Particle Physics and Astronomy Research Council (Brunel and RAL); the Istituto Nazionale di Fisica Nucleare of Italy (Bologna, Ferrara, Frascati, Pisa, Padova, Perugia); and the Japan-US Cooperative Research Project on High Energy Physics (Nagoya, Tohoku).

1 Introduction

The weak couplings of the tau may be studied by investigating the energy spectra of various tau decay products. These spectra are determined by the spin polarization of the taus and the nature of the decay [1].

At the Z^0 , taus are produced with spin polarization due to the inherent parity violation of the Z^0 couplings. At the SLC, this is enhanced due to the electron beam polarization. We can write the production cross sections for left and right handed taus as follows:

$$\begin{aligned}\frac{1}{\sigma_{tot}}\frac{d\sigma_L}{d\cos\theta} &= \tfrac{3}{16}(1+\mathrm{A}_\tau)[(1-\mathrm{A}_e P_e)(1+\cos^2\theta)+2(\mathrm{A}_e-P_e)\cos\theta], \\ \frac{1}{\sigma_{tot}}\frac{d\sigma_R}{d\cos\theta} &= \tfrac{3}{16}(1-\mathrm{A}_\tau)[(1-\mathrm{A}_e P_e)(1+\cos^2\theta)-2(\mathrm{A}_e-P_e)\cos\theta], \qquad (1)\end{aligned}$$

where θ is the polar angle of the τ^- with respect to the incident electron direction, P_e is the electron beam polarization, and A_e and A_τ are the electron and tau parity-violation asymmetry parameters defined as:

$$\mathrm{A}_\ell = \frac{2\hat{g}_v^\ell/\hat{g}_a^\ell}{1+(\hat{g}_v^\ell/\hat{g}_a^\ell)^2}, \qquad (2)$$

where $\hat{g}_v^\ell/\hat{g}_a^\ell$ is the ratio between the effective Z^0 vector and axial-vector couplings to the leptons. The τ^+ are produced in the opposite direction with opposite helicity.

This results in the following expression for the tau polarization as a function of angle and beam polarization:

$$P_\tau(\cos\theta, P_e) = \frac{\frac{d\sigma_R}{d\cos\theta}-\frac{d\sigma_L}{d\cos\theta}}{\frac{d\sigma_R}{d\cos\theta}+\frac{d\sigma_L}{d\cos\theta}} = -\frac{\mathrm{A}_\tau + 2\frac{\mathrm{A}_e-P_e}{1-\mathrm{A}_eP_e}\frac{\cos\theta}{1+\cos^2\theta}}{1+2\mathrm{A}_\tau\frac{\mathrm{A}_e-P_e}{1-\mathrm{A}_eP_e}\frac{\cos\theta}{1+\cos^2\theta}}. \qquad (3)$$

Due to the large beam polarization at SLC, tau polarizations are much higher than at LEP, especially at high $|\cos\theta|$ (see Fig. 1). Also, the polarization of the tau is largely determined by the beam polarization and the production angle, and is relatively unaffected by the Z^0 parity violation.

In this paper, we study the energy spectra of taus decaying to pions, electrons and muons. In the case of the $\tau\to\pi(\mathrm{K})\nu_\tau$ the decay spectrum at rest is mono-energetic, so the boosted energy spectrum directly reflects the angle of the pion in the rest frame. In the case of a three body decay, such as $\tau\to\mu\bar{\nu}_\mu\nu_\tau$ or $\tau\to e\bar{\nu}_e\nu_\tau$, the boosted energy spectrum is a combination of both the rest frame angular distribution and energy spectra. In all of these cases, we can parameterize the decay spectrum in two parts, a constant part that is unaffected by the handedness of the tau, and a

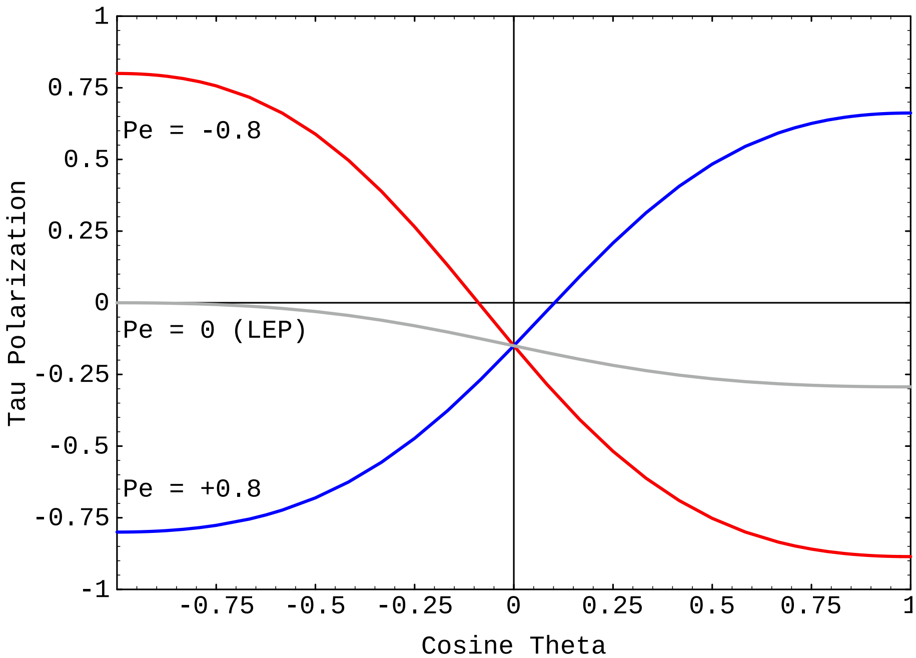

.

Figure 1: Tau polarization vs production angle with and without beam polarization.

polarization- dependent part that changes sign depending on the handedness of the tau:

$$\frac{1}{\Gamma}\frac{d\Gamma_L}{dx} = f(x) + g(x),$$
$$\frac{1}{\Gamma}\frac{d\Gamma_R}{dx} = f(x) - g(x). \tag{4}$$

In the case of the pion or kaon we can describe this with one parameter, h_{ν_τ}, which characterizes the polarization dependent term. We get the following decay spectrum for $\tau \rightarrow \pi(\mathrm{K})\nu_\tau$:

$$f(x) = 1,$$
$$g(x) = \alpha\, \mathrm{h}_{\nu_\tau} \frac{2x - 1 - m_h^2/m_\tau^2}{1 - m_h^2/m_\tau^2}, \tag{5}$$

where m_τ^2 and m_h^2 are the masses of the τ and the decayed hadron respectively, and x is the hadron's energy scaled by the τ energy ($x = \frac{E_h}{E_\mathcal{T}}$). For a spin-0 hadron such as the pion, the analyzing power α has a value of unity.

In the case of the leptons, neglecting mass differences, we can describe the energy spectrum with three Michel parameters[1] ρ, ξ and δ. Here the parameter ρ describes

[1] These parameters were originally conceived to describe muon decay [2]. They describe the energy and the angular spectrum of the resultant electron with respect to the initial muon spin direction. Lepton universality implies that the tau Michel parameters should be identical to the well measured muon Michel parameters [3].

the non-polarization-dependent term, and ξ and δ describe the polarization dependent terms. We get the following spectrum for $\tau \to \ell \bar{\nu}_\ell \nu_\tau$:

$$\begin{aligned} f(x) &= f_1 + \rho \cdot f_2, \\ g(x) &= \xi (g_1 + \delta \cdot g_2), \end{aligned} \tag{6}$$

where

$$\begin{aligned} f_1 &= 2 - 6x^2 + 4x^3, \\ f_2 &= \frac{4}{9}(-1 + 9x^2 - 8x^3), \\ g_1 &= -\frac{2}{3} + 4x - 6x^2 + \frac{8}{3}x^3, \quad \text{and} \\ g_2 &= \frac{4}{9}(1 - 12x + 27x^2 - 16x^3)]. \end{aligned} \tag{7}$$

Here $x = \frac{E_\ell}{E_\mathcal{T}}$.

These decay spectra are combined with the production cross sections to get theoretical decay distributions which can be written as:

$$\frac{1}{\sigma} \frac{d^2\sigma(x, \cos\theta, P_e)}{dx d\cos\theta} = f(x) - P_\mathcal{T}(\cos\theta, P_e) \cdot g(x). \tag{8}$$

Equations 3 through 8 demonstrate the importance of high tau polarization for measuring the polarization dependent terms. For τ^+ decays, the sign of the polarization dependent term is reversed due the opposite helicity of the anti-neutrino. However, since at the Z^0 taus are produced in pairs with opposite helicities, if the τ^- direction is used as the lab frame variable the τ^- and τ^+ decay spectra are identical.

2 Apparatus

The results reported here are based on a sample of 4316 tau-pair candidates collected by the SLC Large Detector (SLD) during the period 1993-1995. The 1993 run accumulated an integrated luminosity of 1.78 pb^{-1} with an average electron beam polarization of 63%, and the 1994-1995 run accumulated 3.66 pb^{-1} with an average polarization of 77%. A general description of the SLD can be found elsewhere [4]. Charged particle tracking and momentum analysis are provided by the Central Drift Chamber (CDC) [5] and the CCD-based vertex detector [6] in a uniform axial magnetic field of 0.6 T. Particle energies are measured in the Liquid Argon Calorimeter (LAC) [7], which is segmented into projective towers with separate electromagnetic and hadronic sections. The measured energy and the shape of the energy flow are used to distinguish between different particles. Additional particle identification is provided by a Čerenkov Ring-Imaging Detector (CRID) [8], and muons are identified and tracked in the Warm Iron Calorimeter (WIC) [9].

The SLD event trigger requires any of several combinations of tracking and energy-flow information from the detector elements. A subset of these have a relatively high efficiency for tau-pair events, in particular a requirement of at least two back-to-back tracks, or a single track plus a minimum energy deposition in the calorimeter.

3 Event Selection

The selection of tau-pair candidates at SLD (for details, see Ref. [10]) is based on the multiplicity, momentum and direction of tracks in the central drift chamber, and on properties of electromagnetic showers in the calorimeter. The event selection efficiency and background contamination were estimated using Monte Carlo. The production of tau-pair events at the Z^0 resonance was simulated using the KORALZ4.0 [11] Monte Carlo generator. The same program was used to generate muon-pair events, while wide-angle Bhabha scattering, two-photon interactions, and multi-hadron final states were produced using the generators described in Refs. [12], [13], and [14], respectively. All these Monte Carlo data samples were subjected to the SLD detector simulation based on the GEANT3.21 [15] program, and to the above event selection. The SLD trigger was also simulated in the Monte Carlo.

Selected tau events are divided into hemispheres by the plane normal to the event thrust axis, and the hemispheres are treated independently. Any pairs of oppositely charged tracks which are consistent with originating from a photon conversion are removed, and hemispheres are then required to have only a single track.

For the selection of tau decays to single pions (or kaons), tracks are required to have no unassociated electromagnetic (EM) LAC energy clusters within $10°$ of the thrust axis. This requirement is powerful for rejecting backgrounds from decays into ρ or a_1. Electrons and muons are rejected by a series of hybrid cuts making use of information from the LAC and WIC. For the tracks that are left, the track momentum must be greater than 3 GeV/c and the total energy in the LAC divided by the track momentum must be less than 0.62. A further requirement of $E_{EM}/p <$ 0.42 is made, and a quasi-invariant mass is calculated assuming that the associated cluster energy originated from photons and that the track is a pion. This quantity is required to be less than 0.3 GeV/c^2. Finally, due to the barrel WIC angular coverage, the remaining tracks are divided into two regions, namely $|\cos\theta| < 0.60$ and $0.60 < |\cos\theta| < 0.74$. The total energy in the LAC divided by the track momentum is required to be greater than 0.14 in the former and 0.31 in the latter case. These criteria discriminate effectively against muons. This selection provides a sample of 573 tracks identified as $\tau \rightarrow \pi(\mathrm{K})\nu_\tau$, with an efficiency of approximately

57% and a purity of 79%. The selection efficiency and background fraction for these decays are plotted in Fig. 2(a) and 2(b) as a function of the scaled energy of the track.

For tau decays to muons, the sample is divided into polar angle regions as above, and tracks are required to have at least one hit in the VXD. In the region of $|\cos\theta| < 0.62$, the WIC is used to identify muons by associating WIC hits with CDC tracks. In the $0.62 < |\cos\theta| < 0.75$ region, shower information from the LAC is used instead. We require that E/p be less than 0.3, that the total number of electromagnetic LAC towers hit in the associated cluster be less than 4, and that there be no unassociated neutral clusters within 20° of the track. In addition, the quasi-invariant mass (calculated as above) is required to be less than 180 MeV/c^2. This results in a sample of 1123 tracks identified as muons, with an estimated selection efficiency 68.9% within the acceptance, and an estimated purity of 98.1%. Fig. 2(c) and 2(d) show the selection efficiency and background fraction for these tracks.

Criteria for selection of tau decays to electrons are the same over the full range $|\cos\theta| < 0.75$, and again one VXD hit is required on all tracks. The LAC shower shape must be consistent with that of an electron, or any valid CRID data must strongly favor the electron hypothesis over the pion hypothesis. We require that no energy be deposited in the back hadronic section of the LAC, and that between 3 and 25 electromagnetic LAC towers be hit in the associated cluster. In addition, if there are no unassociated neutral clusters within 20° of the track, we require that the quasi-invariant mass be less than 500 MeV/c^2. If there are one or two unassociated clusters within 20° of the track, we construct the invariant mass of the cone assuming the track is a pion and the clusters photons, and require this quantity to be less than 500 MeV/c^2. This results in a sample of 932 identified electron tracks with an estimated efficiency of 61.5% within the acceptance and an estimated purity of 98.7%. The efficiency and backgrounds versus scaled energy of these tracks are shown in Fig. 2(e) and 2(f).

4 Data Analysis

As discussed in section 1, and shown in Fig. 1, the average τ polarization depends strongly on production angle and on the sign of the electron beam polarization. The large analyzing power that comes from the SLC beam polarization is clearly illustrated in Fig. 3, where the energy spectrum of $\tau \rightarrow \pi(\mathrm{K})\nu_\tau$ decays is plotted separately for different combinations of these variables. For left-handed incident electrons and τ^- (τ^+) emitted at forward (backward) polar angles, or for right-handed beam and τ^- (τ^+) in the backward (forward) region, the τ^- (τ^+) are predominantly left-handed (right-handed) and the pion energy spectrum is expected to be soft (Fig. 3(a)). For the two opposite combinations of P_e and $\cos\theta$, plotted in Fig. 3(b), the spectrum should be relatively hard since the decaying τ^- (τ^+)

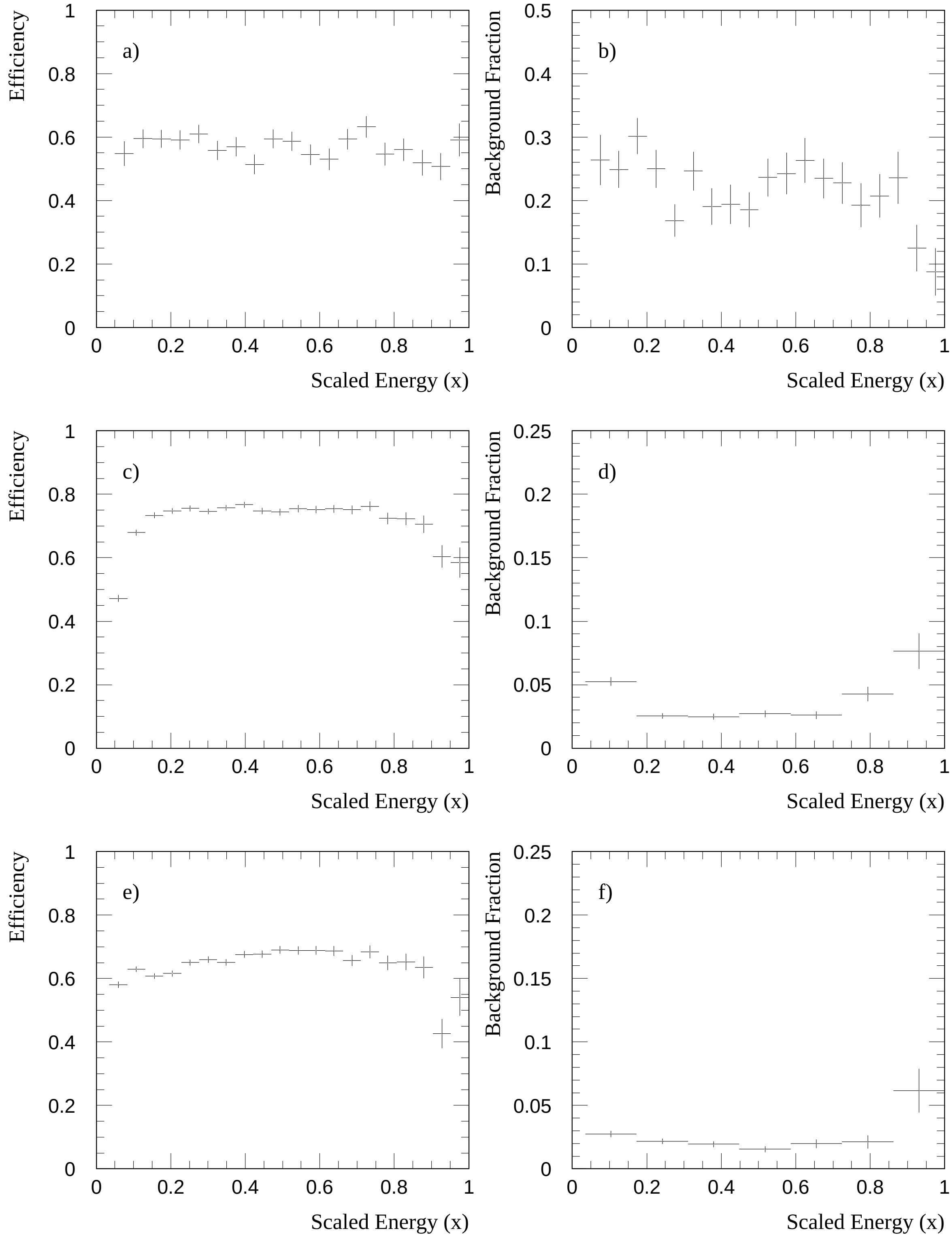

.

Figure 2: The Monte Carlo estimated efficiency and background fractions versus scaled energy for tau decays to pions (a,b), muons (c,d) and electrons (e,f).

are predominantly right-handed (left-handed). The difference is expected to be less obvious for the three-body decays $\tau \to \ell \bar{\nu}_\ell \nu_\tau$, but is still quite visible as shown in Fig. 4.

The tau neutrino helicity, h_{ν_τ}, and the Michel parameters ρ, ξ and $\xi\delta$ are determined using an unbinned maximum likelihood fit to the energy spectra of the decay channels. The fit function is the theoretical differential cross section corrected for radiation and detector effects.

In the maximum likelihood technique, the following expression is minimized:

$$W = -2 \ln \mathcal{L} = -2 \sum_{n=1}^{N} \ln \left\{ \frac{1}{\sigma_i} \frac{d^2\sigma_i}{d\cos\theta \, dx_i} \right\}_n , \tag{9}$$

where $\mathcal{L}$ is the likelihood function. The sum in Eq. 9 runs over all τ's that have been identified as $\tau \to e \bar{\nu}_e \nu_\tau$, $\tau \to \mu \bar{\nu}_\mu \nu_\tau$ or $\tau \to \pi(\mathrm{K}) \nu_\tau$ candidates. The term in the logarithm is the differential cross-section for production of τ-pairs where one τ decays into channel i. This expression is corrected for effects of radiation, detector resolution, efficiency and backgrounds, and is normalized to unity.

The efficiencies and backgrounds were determined from Monte Carlo by studying the distribution of kinematic variables before and after event selection. The dependence of these functions on x and $\cos\theta$ is parameterized using low order polynomials. The radiative correction functions are determined from the ratio of the spectrum generated using KORALZ [11] for events containing radiative effects to the spectrum of events generated with the Born level cross-sections. Since the spectra are different for decays of left- and right-handed taus, the correction functions are divided into four regions corresponding to combinations of positive or negative electron beam polarization and the forward or backward half of the detector. In each region either the left- or right-handed sample is enhanced.

Effects of detector resolution are studied using Monte Carlo for each input variable (e.g. track momentum and direction, thrust axis direction) in bins of that variable From these studies the dependence of the mean and standard deviation are derived as a function of the value of the variable as generated by Monte Carlo, and these functions are used to correct the global resolution distributions. Finally, fits to multiple Gaussians are performed to model both the core and tails of the resolution distributions.

5 Results and Discussion

Fitting the $\tau \to \pi(\mathrm{K}) \nu_\tau$ sample yields a result of $h_{\nu_\tau} = -0.81 \pm 0.18(stat)$, which can be interpreted as the helicity of the tau neutrino. The fit to the $\tau \to \ell \bar{\nu}_\ell \nu_\tau$ channels gives $\xi = 1.03 \pm 0.36(stat)$, $\xi\delta = 0.84 \pm 0.27(stat)$, and $\rho = 0.71 \pm 0.09(stat)$.

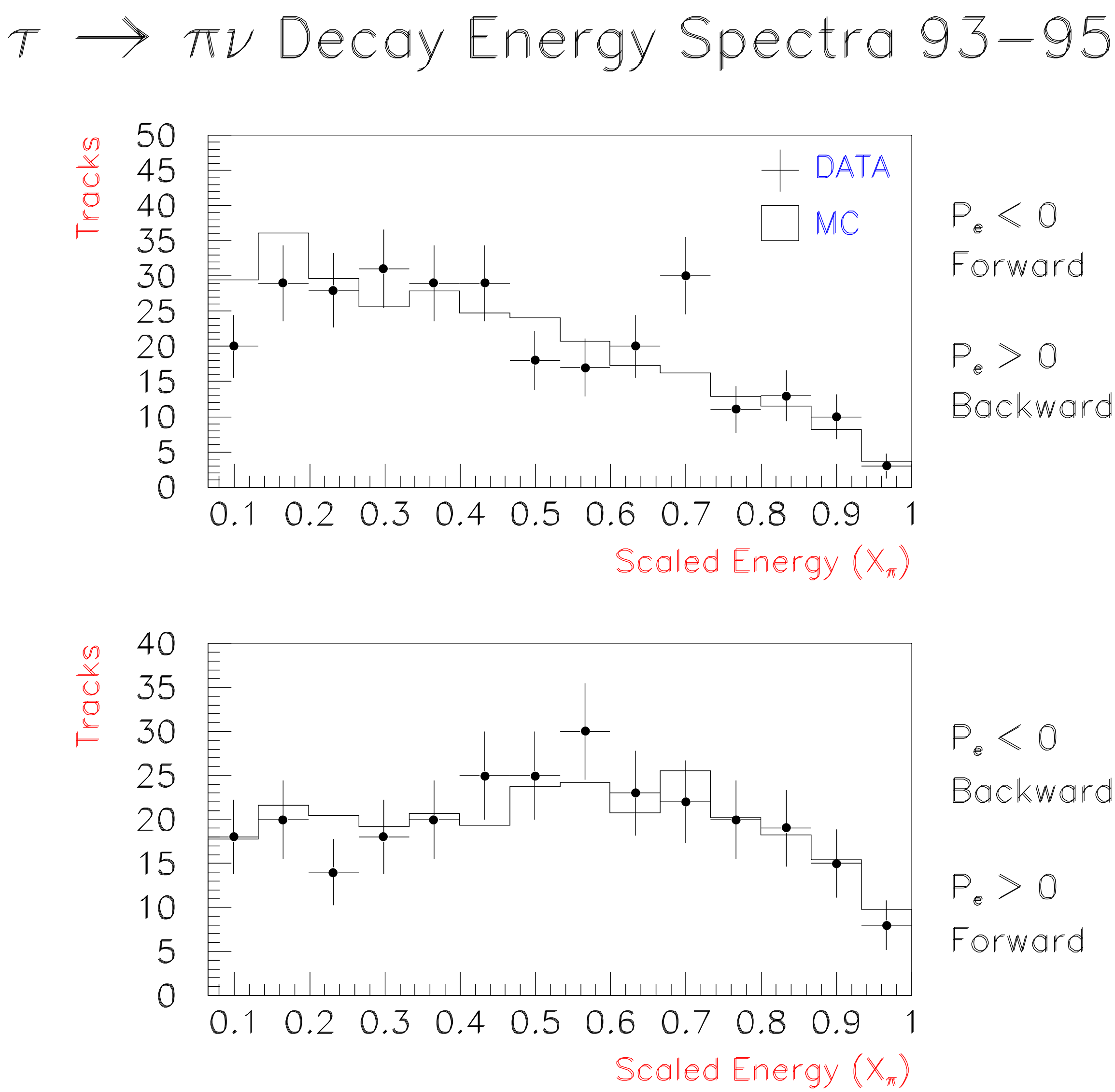

.

Figure 3: $\tau \rightarrow \pi(K)\nu_\tau$ decay energy spectra: (a) The sum of the spectra for pions in the forward direction with beam polarization $P_e < 0$ and in the backward direction with $P_e > 0$; (b) The sum of the spectra for pions in the backward direction with $P_e < 0$ and in the forward direction with $P_e > 0$. In each case the points are data and the histogram is from Monte Carlo.

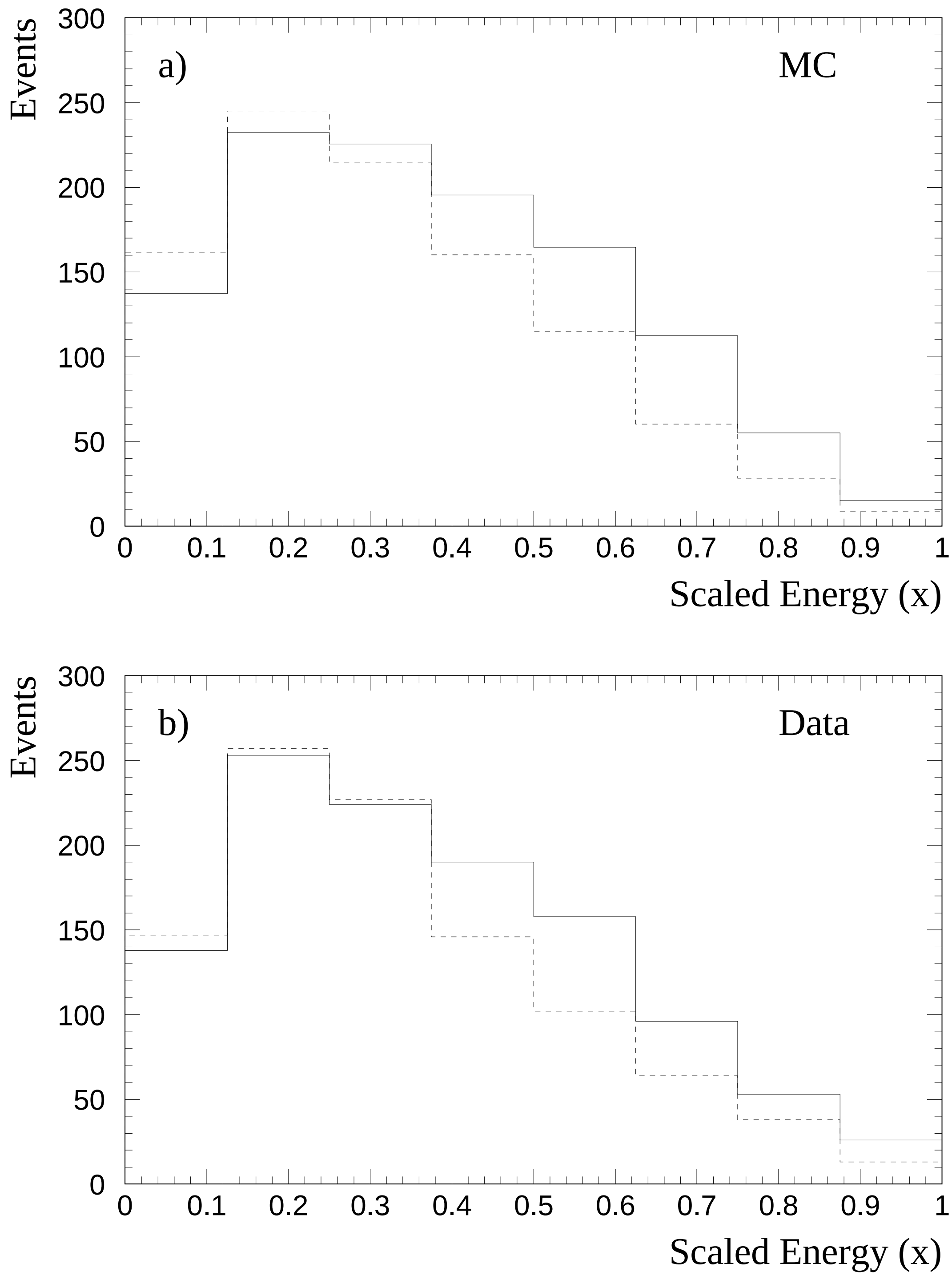

Figure 4: $\tau \rightarrow \ell \bar{\nu}_\ell \nu_\tau$ decay energy spectra from (a) Monte Carlo, and (b) the SLD data. For both histograms, the solid line is the sum of the spectra for leptons in the forward direction with beam polarization $P_e < 0$ and in the backward direction with $P_e > 0$, and the dashed line is the sum of the spectra for leptons in the backward direction with $P_e < 0$ and in the forward direction with $P_e > 0$.

The sources of systematic error which have been considered in the analysis include τ-pair selection efficiency and background, decay identification efficiency and background, resolution in x and $\cos\theta$, uncertainties in the measurements of the beam energy and polarization, uncertainty in the value of A_ℓ [19], and uncertainty in the Mont Carlo estimate of the radiative corrections. Table 1 summarizes the systematic errors in our analysis. To investigate these errors, each parameter used in the fitting programs is modified in turn by its uncertainty, and the fits are redone to obtain new values of h_{ν_τ}, ρ, ξ and $\xi\delta$. Any correlation between these input parameters is taken into account when combining the errors. To estimate the systematic due to radiative corrections, we take ten percent of their effect on the fit values. Where the analysis is not affected by the listed systematic, zero is listed. In particular, for the Michel parameters, a single parameterization is used for the event selection, while for the h_{ν_τ} analysis, this is broken into separate parameterizations for τ selection and final state selection. For the h_{ν_τ} analysis, non-τ background is negligible and contributes nothing to the systematics. The ρ Michel parameter describes the spin-independent part of the lepton spectrum, and is unaffected by beam polarization. Each error listed in Table 1 is a combination of several related contributions, and for the listed errors we assume they are not correlated.

	Δh_{ν_τ}	$\Delta\rho$	$\Delta\xi$	$\Delta(\xi\delta)$
τ selection	0.005	0	0	0
Final-state selection	0.005	0.008	0.032	0.015
τ background	0.011	0.023	0.024	0.033
Non-τ background	0	0.020	0.017	0.007
Radiative corrections	0.015	0.012	0.004	0.005
Resolution	0.013	0.023	0.015	0.023
Beam energy	0	0.013	0.013	0.008
Beam polarization	0.009	0	0.008	0.005
A_e, A_τ	0.007	0.004	0.004	0.008
TOTAL	0.034	0.043	0.049	0.045

Table 1: Systematic uncertainties.

Including systematic errors, the SLD values for h_{ν_τ} and the Michel parameters ρ, ξ and $\xi\delta$ are

$$h_\nu = -0.81 \pm 0.18(stat) \pm 0.03(syst),$$

$$\rho = 0.71 \pm 0.09(stat) \pm 0.04(syst),$$

$$\xi = 1.03 \pm 0.36(stat) \pm 0.05(syst), \quad and$$

$$\xi\delta = 0.84 \pm 0.27(stat) \pm 0.05(syst).$$

These results supersede values presented earlier [16] and are consistent with the Standard Model V-A predictions of -1, $\frac{3}{4}$, 1, $\frac{3}{4}$. The measurements provide an interesting cross check with other experimental results [17], [18], [20] since this analysis does not rely on spin correlations and is the first measurement to be performed with polarized beams. They demonstrate the power of polarized beams for probing deviations from the Standard Model in the weak couplings.

Acknowledgments

We thank the personnel of the SLAC accelerator department and the technical staffs of our collaborating institutions for their outstanding efforts on our behalf.

References

[1] Y.S. Tsai, *Phys. Rev.* **D4** (1971) 2821.

[2] L. Michel, *Proc. Phys. Soc.* **A63** (1950) 514.
C. Bouchiat and L. Michel, *Phys Rev.* **106** (1957) 170.

[3] K.Mursula, M. Roos, F. Scheck, *Nucl. Phys.* **B219** (1989) 321.
W. Fetscher H.J. Gerber, K.F. Johnson, *Phys Lett.* **B173** (1986) 102.

[4] SLD Design Report, SLAC-REPORT-273, May 1984.

[5] M. Fero *et al., Nucl. Instr. Methods* **A367** (1995) 111.

[6] C.J.S. Damerell *et al.,* "Design and Performance of the SLD Vertex Detector, a 120 MPixel Tracking System", Proceedings of the 26th Int. Conf. on High Energy Physics, Dallas, Texas, August 1992;
M. Strauss *et al.,* "Performance of the SLD CCD Pixel Vertex Detector and Design of an Upgrade," Proceedings of the 27th Int. Conf. on High Energy Physics, Glasgow, Scotland, July 1994.

[7] D. Axen *et al., Nucl. Instr. Methods* **A328** (1993) 472.

[8] K. Abe *et al., Nucl. Instr. Methods* **A343** (1994) 74.

[9] A. C. Benvenuti *et al., Nucl. Instr. Methods* **A290** (1990) 353.

[10] SLD Collaboration, K. Abe *et al., Phys. Rev.* **D52** (1995) 4828.

[11] S. Jadach, B.F.L Ward and Z. Was, *Comp. Phys. Comm.* **79** (1994) 503.

[12] H. Anlauf *et al., Comp. Phys. Comm.* **79** (1994) 466.

[13] H. Aihara *et al., Phys. Rev. Lett.* **58** (1987) 97; and references therein.

[14] T. Sjöstrand and M. Bengtsson, *Comp. Phys. Comm.* **43** (1987) 367;
T. Sjöstrand, *Comp. Phys. Comm.* **39** (1986) 347.

[15] GEANT program, version 3.21, CERN Application Software Group, *CERN Program Library* (1994).

[16] M. Daoudi, Proceedings of the International Europhysics Conference on High Energy Physics, Brussels, Belgium, 1995, edited by J. Lemonne, C. Vander Velde, and F. Verbeure (World Scientific Publ., Singapore, 1995), p.625;
K. Abe *et al.,* "Measurement of the τ Charged Weak Couplings with SLC Polarized Beams," SLAC-PUB-95-6971, contributed to the 1995 International Symposium on Lepton and Photon Interactions at High Energies, Beijing, China.

[17] ARGUS collaboration, H. Albrecht *et al., Phys. Lett.* **B337** (1994) 383; *Phys.Lett.* **B349** (1995) 576.

[18] ALEPH Collaboration, D. Buskulic *et al., Phys. Lett.* **B346** (1995) 379.

[19] The SLD asymmetry value $A_\ell = 0.1543 \pm 0.0039$ is used. See E. Torrence, presentation at this conference (ICHEP-96 PA07-063).

[20] CLEO Collaboration, J. Bartelt *et al.,* "$\pi^-\pi^+$ Energy Correlation in τ Pair Events", Proceedings of the 27th Int. Conf. on High Energy Physics, Glasgow, Scotland, July 1994.

**List of Authors

K. Abe,[19] K. Abe,[29] I. Abt,[13] T. Akagi,[27] N.J. Allen,[4] W.W. Ash,[27]†
D. Aston,[27] K.G. Baird,[24] C. Baltay,[33] H.R. Band,[32] M.B. Barakat,[33]
G. Baranko,[9] O. Bardon,[15] T. Barklow,[27] A.O. Bazarko,[10] R. Ben-David,[33]
A.C. Benvenuti,[2] G.M. Bilei,[22] D. Bisello,[21] G. Blaylock,[6] J.R. Bogart,[27]
B. Bolen,[17] T. Bolton,[10] G.R. Bower,[27] J.E. Brau,[20] M. Breidenbach,[27]
W.M. Bugg,[28] D. Burke,[27] T.H. Burnett,[31] P.N. Burrows,[15] W. Busza,[15]
A. Calcaterra,[12] D.O. Caldwell,[5] D. Calloway,[27] B. Camanzi,[11]
M. Carpinelli,[23] R. Cassell,[27] R. Castaldi,[23][a] A. Castro,[21]
M. Cavalli-Sforza,[6] A. Chou,[27] E. Church,[31] H.O. Cohn,[28] J.A. Coller,[3]
V. Cook,[31] R. Cotton,[4] R.F. Cowan,[15] D.G. Coyne,[6] G. Crawford,[27]
A. D'Oliveira,[7] C.J.S. Damerell,[25] M. Daoudi,[27] R. De Sangro,[12]
R. Dell'Orso,[23] P.J. Dervan,[4] M. Dima,[8] D.N. Dong,[15] P.Y.C. Du,[28]
R. Dubois,[27] B.I. Eisenstein,[13] R. Elia,[27] E. Etzion,[4] D. Falciai,[22] C. Fan,[9]
M.J. Fero,[15] R. Frey,[20] K. Furuno,[20] T. Gillman,[25] G. Gladding,[13]
S. Gonzalez,[15] G.D. Hallewell,[27] E.L. Hart,[28] J.L. Harton,[8] A. Hasan,[4]
Y. Hasegawa,[29] K. Hasuko,[29] S. J. Hedges,[3] S.S. Hertzbach,[16]
M.D. Hildreth,[27] J. Huber,[20] M.E. Huffer,[27] E.W. Hughes,[27] H. Hwang,[20]
Y. Iwasaki,[29] D.J. Jackson,[25] P. Jacques,[24] J. A. Jaros,[27] A.S. Johnson,[3]
J.R. Johnson,[32] R.A. Johnson,[7] T. Junk,[27] R. Kajikawa,[19] M. Kalelkar,[24]
H. J. Kang,[26] I. Karliner,[13] H. Kawahara,[27] H.W. Kendall,[15] Y. D. Kim,[26]
M.E. King,[27] R. King,[27] R.R. Kofler,[16] N.M. Krishna,[9] R.S. Kroeger,[17]
J.F. Labs,[27] M. Langston,[20] A. Lath,[15] J.A. Lauber,[9] D.W.G.S. Leith,[27]
V. Lia,[15] M.X. Liu,[33] X. Liu,[6] M. Loreti,[21] A. Lu,[5] H.L. Lynch,[27] J. Ma,[31]
G. Mancinelli,[22] S. Manly,[33] G. Mantovani,[22] T.W. Markiewicz,[27]
T. Maruyama,[27] H. Masuda,[27] E. Mazzucato,[11] A.K. McKemey,[4]
B.T. Meadows,[7] R. Messner,[27] P.M. Mockett,[31] K.C. Moffeit,[27]
T.B. Moore,[33] D. Muller,[27] T. Nagamine,[27] S. Narita,[29] U. Nauenberg,[9]
H. Neal,[27] M. Nussbaum,[7] Y. Ohnishi,[19] L.S. Osborne,[15] R.S. Panvini,[30]
H. Park,[20] T.J. Pavel,[27] I. Peruzzi,[12][b] M. Piccolo,[12] L. Piemontese,[11]
E. Pieroni,[23] K.T. Pitts,[20] R.J. Plano,[24] R. Prepost,[32] C.Y. Prescott,[27]
G.D. Punkar,[27] J. Quigley,[15] B.N. Ratcliff,[27] T.W. Reeves,[30] J. Reidy,[17]
P.E. Rensing,[27] L.S. Rochester,[27] P.C. Rowson,[10] J.J. Russell,[27]
O.H. Saxton,[27] T. Schalk,[6] R.H. Schindler,[27] B.A. Schumm,[14] S. Sen,[33]
V.V. Serbo,[32] M.H. Shaevitz,[10] J.T. Shank,[3] G. Shapiro,[14] D.J. Sherden,[27]
K.D. Shmakov,[28] C. Simopoulos,[27] N.B. Sinev,[20] S.R. Smith,[27] M.B. Smy,[8]
J.A. Snyder,[33] P. Stamer,[24] H. Steiner,[14] R. Steiner,[1] M.G. Strauss,[16]
D. Su,[27] F. Suekane,[29] A. Sugiyama,[19] S. Suzuki,[19] M. Swartz,[27]
A. Szumilo,[31] T. Takahashi,[27] F.E. Taylor,[15] E. Torrence,[15] A.I. Trandafir,[16]
J.D. Turk,[33] T. Usher,[27] J. Va'vra,[27] C. Vannini,[23] E. Vella,[27]
J.P. Venuti,[30] R. Verdier,[15] P.G. Verdini,[23] S.R. Wagner,[27] A.P. Waite,[27]
S.J. Watts,[4] A.W. Weidemann,[28] E.R. Weiss,[31] J.S. Whitaker,[3]
S.L. White,[28] F.J. Wickens,[25] D.A. Williams,[6] D.C. Williams,[15]

S.H. Williams,[27] S. Willocq,[33] R.J. Wilson,[8] W.J. Wisniewski,[27]
M. Woods,[27] G.B. Word,[24] J. Wyss,[21] R.K. Yamamoto,[15] J.M. Yamartino,[15]
X. Yang,[20] S.J. Yellin,[5] C.C. Young,[27] H. Yuta,[29] G. Zapalac,[32]
R.W. Zdarko,[27] C. Zeitlin,[20] and J. Zhou,[20]

[1]*Adelphi University, Garden City, New York 11530*
[2]*INFN Sezione di Bologna, I-40126 Bologna, Italy*
[3]*Boston University, Boston, Massachusetts 02215*
[4]*Brunel University, Uxbridge, Middlesex UB8 3PH, United Kingdom*
[5]*University of California at Santa Barbara, Santa Barbara, California 93106*
[6]*University of California at Santa Cruz, Santa Cruz, California 95064*
[7]*University of Cincinnati, Cincinnati, Ohio 45221*
[8]*Colorado State University, Fort Collins, Colorado 80523*
[9]*University of Colorado, Boulder, Colorado 80309*
[10]*Columbia University, New York, New York 10027*
[11]*INFN Sezione di Ferrara and Università di Ferrara, I-44100 Ferrara, Italy*
[12]*INFN Lab. Nazionali di Frascati, I-00044 Frascati, Italy*
[13]*University of Illinois, Urbana, Illinois 61801*
[14]*Lawrence Berkeley Laboratory, University of California, Berkeley, California 94720*
[15]*Massachusetts Institute of Technology, Cambridge, Massachusetts 02139*
[16]*University of Massachusetts, Amherst, Massachusetts 01003*
[17]*University of Mississippi, University, Mississippi 38677*
[19]*Nagoya University, Chikusa-ku, Nagoya 464 Japan*
[20]*University of Oregon, Eugene, Oregon 97403*
[21]*INFN Sezione di Padova and Università di Padova, I-35100 Padova, Italy*
[22]*INFN Sezione di Perugia and Università di Perugia, I-06100 Perugia, Italy*
[23]*INFN Sezione di Pisa and Università di Pisa, I-56100 Pisa, Italy*
[24]*Rutgers University, Piscataway, New Jersey 08855*
[25]*Rutherford Appleton Laboratory, Chilton, Didcot, Oxon OX11 0QX United Kingdom*
[26]*Sogang University, Seoul, Korea*
[27]*Stanford Linear Accelerator Center, Stanford University, Stanford, California 94309*
[28]*University of Tennessee, Knoxville, Tennessee 37996*
[29]*Tohoku University, Sendai 980 Japan*
[30]*Vanderbilt University, Nashville, Tennessee 37235*
[31]*University of Washington, Seattle, Washington 98195*
[32]*University of Wisconsin, Madison, Wisconsin 53706*
[33]*Yale University, New Haven, Connecticut 06511*
†*Deceased*
[a]*Also at the Università di Genova*
[b]*Also at the Università di Perugia*